

Numerical Modelling of Emission Characteristic for a Single Cylinder Spark Ignition Engine

Brahim MENACER**, Khatir NAIMA**, Mostefa BOUCHETARA*****

*Higher School of Electrical Engineering and Energetics ESGEE Oran, Chemin Vicinal N9, Oran 31000, Algeria, E-mail: acer.msn@hotmail.fr (Corresponding author)

**Department of technology, BP: 66, University Centre of Naama, Naama 45000, Algeria, E-mail: knaima@cuniv-naama.dz

***Laboratory of Gas Combustion and Environment Department of Mechanical Engineering, University of Sciences and the Technology of Oran, L.P 1505 El -Menaouer, USTO 31000 Oran, Algeria, E-mail: mbouchetara@hotmail.com

crossref <http://dx.doi.org/10.5755/j02.mech.31064>

1. Introduction

Due to strict exhaust gas regulations, much of the current research in internal combustion engine development is directed toward reducing emissions of particulates and nitrogen oxides to protect the environment [1]. So far, there are two main methods (empirical and theoretical) to improve performance and minimize emissions from internal combustion engines. Empirical methods give better results, but these methods can cost more than theoretical models and require more time on the design and testing side of new systems [2].

Generally, there are two models to do the mathematical simulation of internal combustion engines, the models based on fluid dynamics, which are based on the three Navies Stokes equations, and the thermodynamic models, which are based on the application of the 1st and 2nd laws of thermodynamics to an open system of air-fuel mixture and residual gas in the manifolds and cylinders. Several researchers studied the effect of both parameters (compression ratio and equivalence ratio) on emissions in internal combustion engines, including the spark ignition engine [3]. Ahmet A.Y. et al. [4] studied the equivalence ratio effect on engine emissions by using three types of gasoline fuels; CNG, gasoline, and G9C1 (CNG mixture). The type of G9C1 was found to have the lowest level of CO, followed by CNG and gasoline. NOx emissions are higher in the G9C1 (the maximum values of NOx are 0.0098 for CNG, 0.0070 for G9C1, and 0.0043 for gasoline). Ahmadipour S. [5] studied the effect of the compression ratio and the type of injected fuels (diesel and B100) on the performance and emissions of the turbocharged diesel engine. It was found that CO and CO2 emissions are higher in diesel fuel by comparing B100 fuel, while soybean biodiesel (B100) emitted more NOx. Maher A.R. et al. [6] developed a numerical simulation program to study the effect of engine parameters such as compression ratio, equivalence ratio, and engine speed on the main performances (power, torque, and specific consumption) and NOx emissions from a carbureted hydrogen engine. It's shown that the compression ratio and the equivalence ratio have a remarkable effect on the performance and emissions of the engine. It must make a particular choice of these two parameters to have better engine performance. Gupta, S.K. et al. [7] evaluated the impact of the compression ratio on the combustion parameters and emission of a spark-ignition engine for several operating conditions. The results showed that if the engine is running with

a low load (about 5 Nm) and if the compression ratio increases by a value of 1.7 (from 6.7: 1 to 9.4: 1), then the thermal efficiency increases by a value of 3.1% (from 9.8% to 12.9%) and CO emissions decrease. For a compression ratio of 9: 1, then power and thermal efficiency are maximum, while the average effective pressure and specific fuel consumption are lower [8]. Considering the literature review, it has been noticed that the effect of compression ratio and equivalence ratio on the emission characteristics of SI engine with a two-zone model has not extensively been investigated. In this paper, the engine simulation model is based on a two-zone thermodynamic model to characterize each engine cycle phase to predict relevant spark engine emissions.

2. Modeling engine equations

To build the two-zone combustion model, we have chosen to make some simplifications in this article:

- ✓ In the two-zone combustion model, the combustion chamber is divided into two zones (burnt and unburnt) which are assumed to be spatially homogeneous [9]. These two zones are separated by a flame front (see Fig. 1).
- ✓ In the engine cycle and during the compression period, the model is considered single-zone (homogeneous mixture) and no pre-flame reaction.
- ✓ The case of ideal gases was taken as a hypothesis for all calculations of the periods of the engine cycle (intake, compression, combustion-expansion and exhaust).
- ✓ No heat transfer between the two zones (burnt and unburnt) [10]. Each of these zones is considered to be thermally insulating.
- ✓ For the two manifolds (intake and exhaust), the pressure and the temperature of the gases are considered constant.
- ✓ We neglected the valve leakage and blow-by in this article.

The energy conservation, ideal gas and mass conservation equations are used in the two-zone combustion model [11]: The cylinder total mass of gas is given by:

$$m = m_b + m_u. \quad (1)$$

For the two-zone combustion model, the sum of the volumes of the two zones (burned and unburnt) gives the total volume of the combustion chamber:

$$V = V_b + V_u. \quad (2)$$

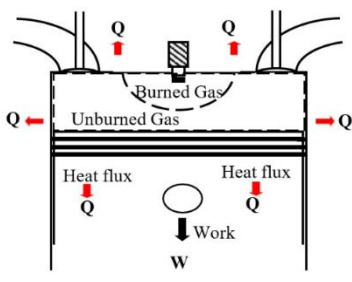


Fig. 1 Spark engine using dual-zone combustion model

For each combustion zone, the equation of state of the ideal gas is:

$$\begin{cases} P \cdot V_u = m_u \cdot R_u \cdot T_u \\ P \cdot V_b = m_b \cdot R_b \cdot T_b \end{cases} \quad (3)$$

For each combustion zone (burnt and unburned), the pressure and temperature equations are [12]:

$$\frac{dP}{d\theta} = \frac{A+B+C}{D+E}, \quad (4)$$

$$\begin{aligned} \frac{dT_b}{d\theta} = & \frac{-h(\pi b^2/2 + 4V/b)x^{0.5}T_b - T_w}{vmc_{p,b}x} + \frac{v_b}{c_{p,b}} \left(\frac{\partial \ln v_b}{\partial \ln T_b} \right) \times \\ & \times \left(\frac{dP}{d\theta} \right) + \frac{h_u - h_b}{xc_{p,b}} \left[\frac{dx}{d\theta} - x - x^2 \frac{C}{\omega} \right], \end{aligned} \quad (5)$$

$$\begin{aligned} \frac{dT_u}{d\theta} = & \frac{-h(\pi b^2/2 + 4V/b)x^{0.5}T_u - T_w}{vmc_{p,u}x} + \frac{v_u}{c_{p,u}} \left(\frac{\partial \ln v_u}{\partial \ln T_u} \right) \times \\ & \times \left(\frac{dP}{d\theta} \right) + \frac{h_u - h_b}{xc_{p,u}} \left[\frac{dx}{d\theta} - x - x^2 \frac{C}{\omega} \right]. \end{aligned} \quad (6)$$

The constants A, B, C, D, E are calculated by using of Olikara and Borman model [13]:

$$A = \frac{1}{m} \left(\frac{dV}{d\theta} + \frac{VC}{\omega} \right), \quad (7)$$

$$B = h \frac{A}{\omega} \times \left[\frac{v_b}{c_{p,b}} \frac{\partial \ln v_b}{\partial \ln T_b} x^{0.5} \frac{T_b - T_w}{T_b} + \frac{v_u}{c_{p,u}} \frac{\partial \ln v_u}{\partial \ln T_u} (1 - x^{0.5}) \frac{T_u - T_w}{T_u} \right], \quad (8)$$

$$C = -v_b - v_u \frac{dx}{d\theta} - \frac{v_b}{c_{p,b}} \frac{\partial \ln v_b}{\partial \ln T_b} x^{0.5} \frac{h_u - h_b}{T_b} \left[\frac{dx}{d\theta} - \frac{(x-x^2)C}{\omega} \right], \quad (9)$$

$$D = x \left[\frac{v_b^2}{T_b c_{p,b}} \left(\frac{\partial \ln v_u}{\partial \ln T_u} \right)^2 + \frac{v_b}{P} \frac{\partial \ln v_b}{\partial \ln P} \right], \quad (10)$$

$$E = 1 - x \left[\frac{v_u^2}{T_u c_{p,u}} \left(\frac{\partial \ln v_u}{\partial \ln T_u} \right)^2 + \frac{v_u}{P} \frac{\partial \ln v_u}{\partial \ln P} \right]. \quad (11)$$

Based on the fact that the pressure of burnt and unburnt gases is the same, v_b and v_u depend on T_b, T_u and P . So we can replace the logarithmic derivatives of Depcik's model [14], we find:

$$\frac{\partial v_b}{\partial \theta} = \frac{v_b}{T_b} \frac{\partial \ln v_b}{\partial \ln T_b} \frac{dT_b}{d\theta} + \frac{v_b}{P} \frac{\partial \ln v_b}{\partial \ln P} \frac{dP}{d\theta}, \quad (12)$$

$$\frac{\partial v_u}{\partial \theta} = \frac{v_u}{T_u} \frac{\partial \ln v_u}{\partial \ln T_u} \frac{dT_u}{d\theta} + \frac{v_u}{P} \frac{\partial \ln v_u}{\partial \ln P} \frac{dP}{d\theta}. \quad (13)$$

Starting from the same pressure assumption and including the logarithmic derivatives, the internal energies of the burnt and unburnt gases can give as follows:

$$\frac{\partial u_b}{\partial \theta} = \left(c_{pb} - \frac{pv_b}{T_b} \frac{\partial \ln v_b}{\partial \ln T_b} \right) \frac{dT_b}{d\theta} - v_b \left(\frac{\partial \ln v_b}{\partial \ln T_b} + \frac{\partial \ln v_b}{\partial \ln P} \right) \frac{dP}{d\theta}, \quad (14)$$

$$\frac{\partial u_u}{\partial \theta} = \left(c_{pu} - \frac{pv_u}{T_u} \frac{\partial \ln v_u}{\partial \ln T_u} \right) \frac{dT_u}{d\theta} - v_u \left(\frac{\partial \ln v_u}{\partial \ln T_u} + \frac{\partial \ln v_u}{\partial \ln P} \right) \frac{dP}{d\theta}. \quad (15)$$

The heat loss of the gases for the two zones (burned and unburned) depends on the rate of change of the specific entropy. Its expression is given by [15]:

$$-\dot{Q}_b = mwxT_b \frac{dS_b}{d\theta}, \quad (16)$$

$$-\dot{Q}_u = mw(1-x)T_u \frac{dS_u}{d\theta}, \quad (17)$$

where:

$$\frac{dS_b}{d\theta} = \left(\frac{c_{pb}}{T_b} \right) \frac{dT_b}{d\theta} - \frac{v_b}{T_b} \frac{\partial \ln v_b}{\partial \ln T_b} \frac{dP}{d\theta}, \quad (18)$$

$$\frac{dS_u}{d\theta} = \left(\frac{c_{pu}}{T_u} \right) \frac{dT_u}{d\theta} - \frac{v_u}{T_u} \frac{\partial \ln v_u}{\partial \ln T_u} \frac{dP}{d\theta}. \quad (19)$$

The mixture state is given by the following equation [16]:

$$\frac{du}{d\theta} = \left(c_p - \frac{Pv}{T} \frac{\partial \ln v}{\partial \ln T} \right) \frac{dT}{d\theta} - \left(v \left(\frac{\partial \ln v}{\partial \ln T} + \frac{\partial \ln v}{\partial \ln P} \right) \right) \frac{dP}{d\theta}, \quad (20)$$

$$\frac{dv}{d\theta} = \frac{v}{T} \frac{\partial \ln v}{\partial \ln T} \frac{dT}{d\theta} - \frac{v}{P} \frac{\partial \ln v}{\partial \ln P} \frac{dP}{d\theta}, \quad (21)$$

$$\frac{ds}{d\theta} = \frac{c_p}{T} \frac{dT}{d\theta} - \frac{v}{T} \frac{\partial \ln v}{\partial \ln T} \frac{dP}{d\theta}, \quad (22)$$

$$\frac{dW}{d\theta} = P \frac{dV}{d\theta}. \quad (23)$$

During a modelization with only one fuel [17], the equivalence ratio is calculated by:

$$\Phi = \left(\frac{[F]}{air} \right)_{act} / \left(\frac{[F]}{air} \right)_{st} \quad (24)$$

3. Modeling of heat transfer in the combustion chamber:

This investigation takes into account only the heat transfer by convection. Heat transfer by radiation and by conduction through the walls are neglected. Newton's equation is used to calculate the heat flux from the in-cylinder gas to the combustion chamber walls [18]:

$$\frac{dQ_w(\theta)}{d\theta} = \frac{1}{6.n} \times h(\theta).A_w(\theta).(T_g(\theta) - T_w), \quad (25)$$

where: $\frac{dQ_w(\theta)}{d\theta}$ snapshot convective heat transfer rate;

$A_w(\theta)$ is napsnot wall area; $T_g(\theta)$ is Snapshot gas temperature; T_w is cylinder wall temperature; $h(\theta)$ is instantaneous local mean heat transfer coefficient; n is engine speed.

The instantaneous local mean heat transfer coefficient $h(\theta)$ for the cylinder is given by the Woschni correlation [19]:

$$h(\theta) = 130.D^{-0.2}.T_g^{-0.53}.p_g^{0.8}.v_g^{0.8}. \quad (26)$$

The average cylinder gas velocity v_g is calculated as:

$$v_g = k_1.c_m + k_2 \left(\frac{V_d T_1}{p_1 V_1} \right) \left[p_g - p_1 \left(\frac{V_1}{V_g} \right)^k \right], \quad (27)$$

where: c_m the average piston speed; V_d the displacement volume; p_1, T_1, V_1 the reference pressure, temperature, and volume, respectively; k_1 and k_2 are coefficients that depend on the stroke of the engine cycle. k_1 has a value of 6.18 for the gas exchange phase and a value of 2.28 for compression, combustion, and expansion. k_2 has a value of 3.24×10^{-3} for the combustion and expansion periods and a zero value ($k_2 = 0$) for the other strokes of the engine cycle [20].

In This paper, we take into consideration the phenomenon of heat transfer between the gas and the walls of the intake and exhaust manifolds in the cylinder head. The heating fresh gas mixture phenomenon on the intake side is not neglected. However, the calculation of the fill rate would be too high. For the exhaust side, the heat transfer of the burnt gases to the wall of the exhaust manifold is also taken into account so as not to have excessively high exhaust gas temperatures. Using the Zapf approach to determine the heat transfer coefficient [21].

The heat transfer coefficient in the case of the inlet channel is given by:

$$h_{i,c} = 2,1515. \left(1 - 0,765. \frac{e_{v,i}}{d_{v,o}} \right) \dot{m}_i^{0,68} . T_1^{-0,28} . D_i^{-1,68}, \quad (28)$$

and for the outlet channel:

$$h_{o,c} = 1,79102. \left(1 - 0,770. \frac{e_{o,v}}{d_{o,v}} \right) \dot{m}_o^{0,5} . T_1^{0,41} . D_o^{-1,5}, \quad (29)$$

where: $h_{i,c}, h_{o,c}$ is valve lift; \dot{m} is mass flow; T_1 is gas temperature at inlet channel; d_v is inner valve seat diameter; D_i, D_o are average channel diameter.

4. Configuration of the developed engine simulation program

GT-Suite software is a simulation tool for modeling internal combustion engines' combustion. In the current study, GT-Suite is used to investigate the combustion behavior and the emissions characteristics in a four-stroke spark-ignition engine with a single cylinder and fuel injection. The characteristics of this engine are presented in Table 1. The GT-Suite engine software allows the user to model an internal combustion engine using the predefined elements provided in the software toolbox. Connectors connect the various components to establish the complete motor model. The simulation model developed with the GT-Suite engine software is shown in Fig. 2.

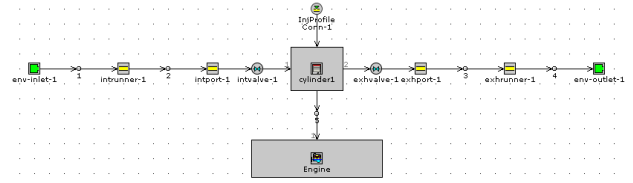


Fig. 2 Spark engine model with GT-Power software

5. Results and discussions

Table 1 gives the main engine specifications and operating conditions to simulate the results for a single-cylinder direct injection spark ignition engine.

Table 1

Main spark Engine specifications

Parameters and units	Values
Bore, mm	80.6
Stroke, mm	88
Connecting road, mm	300
Compression ratio, -	9.1
Cylinder number, -	01
Injection timing, BTDC	10°
Intake valve opens, BTDC	11°
Intake valve closes, ABDC	32°
Exhaust valve opens, BBDC	35°
Exhaust valve closes, ATDC	16°

Fig. 3 shows the cylinder pressure curve obtained using the GT-Power simulation software at full load and engine speed of 3600 rpm for a compression ratio of 9:1 and equivalence ratio of 0.9. We used the experimental cylinder pressure of Smin et al [22] to validate our simulation model. There is a good agreement between the simulation and the experimental result.

Fig. 4 represents the variation of the in-cylinder gas temperature as a function of the crankshaft angle in the two zones (burnt and unburnt), engine speed of 1600 rpm, at full load and for two engine equivalence ratios (ER = 0.8 and 0.9). A very rapid increase in temperature of the burning zone with the start of combustion is depicted. The high burning zone temperature is responsible for the formation of NO and soot. And on the other hand, a slight change in temperature in the unburned zone.

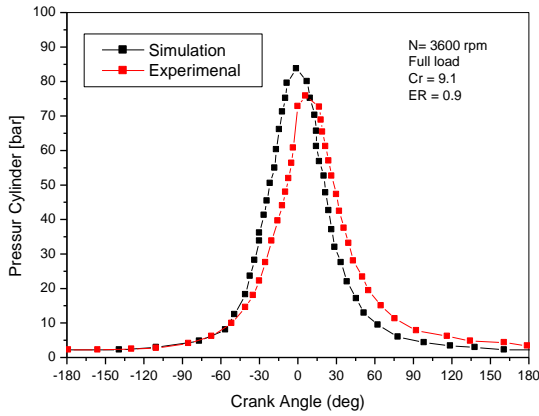


Fig. 3 Experimental and theoretical results comparison of in-cylinder pressure versus crank angle [22]

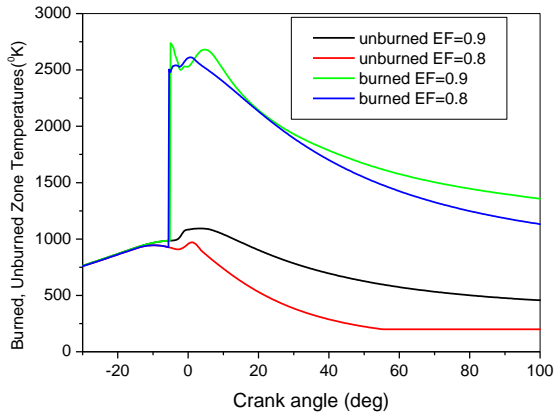


Fig. 4 Two zones combustion chamber temperature versus crank angle

5.1. Influence of the compression ratio on the NOx

The effect of the compression ratio on the NOx for different engine speed is shown in Fig. 5. The NOx decrease with the increase of the compression ratio and the engine speed. At an engine speed of 1800 rpm, if the compression increases by 2 (from 9:1 to 11:1) so the NOx decreases by 7%.

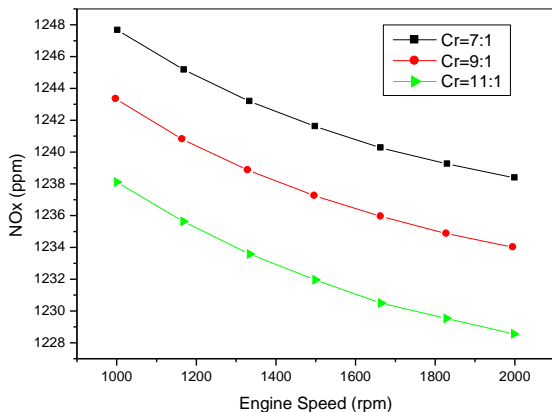


Fig. 5 NOx versus engine speed variation for different values of compression ratio at full load

5.2. Effect of compression ratio on the carbon monoxide emission (CO)

Fig. 6 shows the compression ratio effect on the CO for different engine speeds. The CO increases with the

compression ratio and decreases with the engine speed increase. At an engine speed of 1800 rpm, if the compression increases by 2 (from 9:1 to 11:1), the CO increases by 3%.

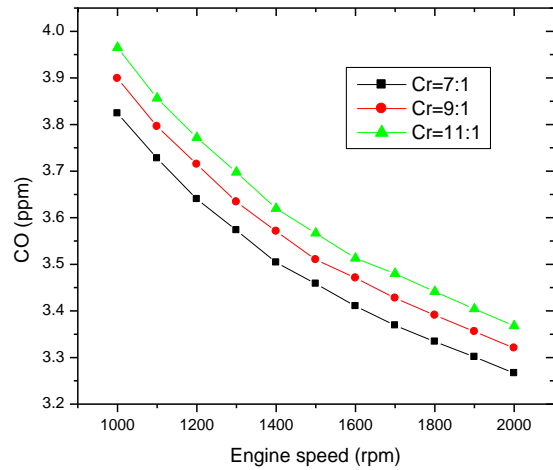


Fig. 6 Carbon monoxide emission (CO) versus engine speed variation for different values of compression ratio

5.3. Influence of the compression ratio on the HC

Fig. 7 show the effect of the compression ratio on the CO for different engine speed. The HC increase with the compression ratio and decrease with the increase of the engine speed. At an engine speed of 1800 rpm, if the compression increases by 2 (from 9:1 to 11:1) so the HC increase by 4 %.

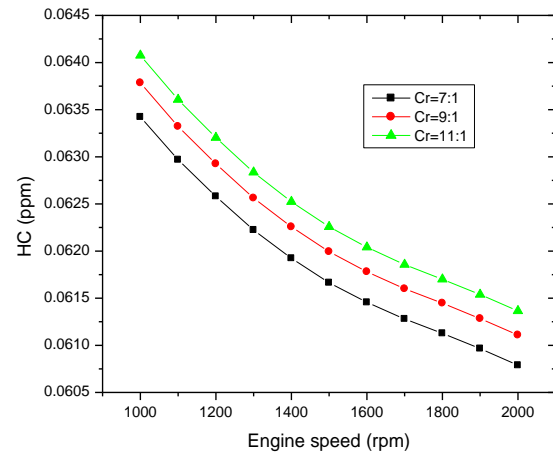


Fig. 7 Hydrocarbon emission (HC) versus engine speed variation for different values of compression ratio

5.4. Effect of equivalence ratio on the NOx emission

The effect of the equivalence ratio on the NOx for different compression ratios is shown in Figure 8. The NOx increases with the equivalence ratio and decreases with the compression ratio increase. At an engine speed of 1800 rpm, if the equivalence ratio increases by 1 (from 0.8 to 0.9), the NOx increases by 6%.

5.5. Influence of the equivalence ratio on the CO

The effect of the equivalence ratio on the CO for different engine speed is shown in Figure 9. The CO increases with the compression ratio and decreases with the equivalence ratio increase. At an engine speed of 1800 rpm,

if the equivalence ratio increases by 1 (from 0.8 to 0.9), the CO decreases by 4%.

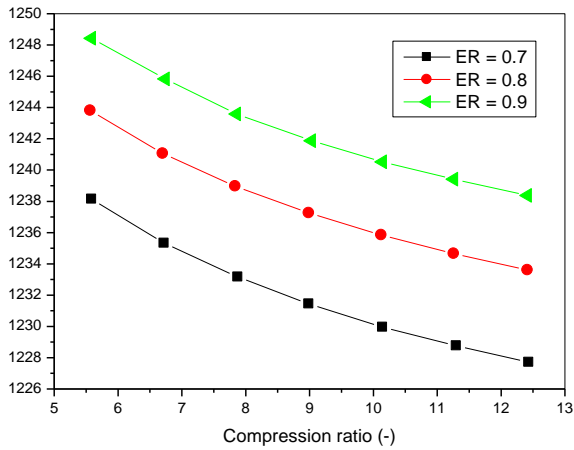


Fig. 8 NOx versus compression ratio variation for different values of equivalence ratio

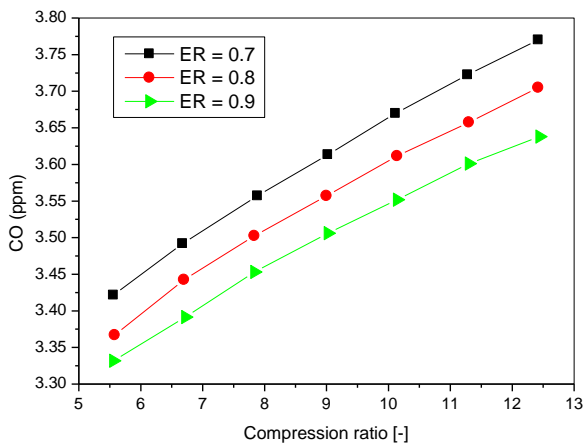


Fig. 9 CO versus compression ratio variation for different values of equivalence ratio

5.6. Influence of the equivalence ratio on the HC

The effect of the equivalence ratio on the HC for different engine speed is shown in Fig. 10. The HC increases with the compression ratio and decreases with the equivalence ratio increase. At an engine speed of 1800 rpm, if the equivalence ratio increases by 1 (from 0.8 to 0.9), the HC decreases by 5%.

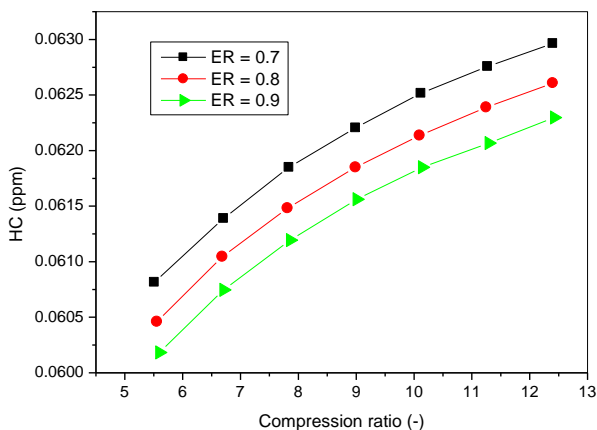


Fig. 10 HC versus compression ratio variation for different values of equivalence ratio

6. Conclusion

The paper attempts to shed some light on the effect of compression ratio and equivalence ratio on the main emissions of the direct injection spark engine. The thermodynamic cycle program uses the two-zone combustion analytical model to study the spark engine emissions such as hydrocarbons, carbon monoxide, and nitrogen oxides. The model is constructed by using of the GT-Suite simulation software. Through experimental tests and the GT-Power commercial software, it was possible to evaluate the effect of the various engine parameters (such as compression ratio and equivalence ratio) on the main emissions characteristics of the investigated engine. Based on the computational studies in predicting the heat transfer of the diesel engine, it can be concluded that:

- ✓ The comparison between the developed analytical model and experimental data for the in-cylinder pressure shows an acceptable agreement for both results. So our simulation program is validated by this comparison.
- ✓ The compression and equivalence ratios have a remarkable effect on the spark ignition engine emissions results. These two parameters must be considered to obtain better performance characteristics from the engine.

By considering a multi-zone combustion model instead of a two-zone model, we will be able to predict the engine's behavior in terms of engine performance and pollutant emissions.

Acknowledgment

This study was performed under the framework of 'Projet Impact Socio-Economique' Contract N° 362 funded by the General Directorate of Algerian Scientific Research (DGRSDT).

References

1. Zareei, J.; Kakaee, A. H. 2013. Study and the effects of ignition timing on gasoline engine performance and emissions, Euro. Trans. Res. Rev. 5(2): 109-116. <https://doi.org/10.1007/s12544-013-0099-8>.
2. Heywood, J. B. 1988. Internal combustion engine fundamentals, McGraw-Hill, New York 1:135-164. [http://dx.doi.org/10.1016/S0082-0784\(75\) 80383-3](http://dx.doi.org/10.1016/S0082-0784(75) 80383-3).
3. Binjuwair, S. A.; et al. 2017. Combustion and emission analysis of si engine fuelled by saudi arabian gasoline RON91 and RON95 with variable compression ratios and spark timing, Open Access Library Journal 4: e4184. <https://doi.org/10.4236/oalib.1104184>.
4. Ahmet, A. Y.; Yahya, D. 2019. Effects of equivalence ratio and CNG addition on engine performance and emissions in a dual sequential ignition engine, International journal of Engine Research 1-16. <https://doi.org/10.1177%2F1468087419834190>.
5. Ahmadipour, S.; Aghkhani, M. H.; et al. 2019. The effect of compression ratio and alternative fuels on performance and exhaust emission in a diesel engine by modelling engine, AUT J. Mech. Eng. 3(2): 217-228. <http://dx.doi.org/10.22060/ajme.2019.15162.5764>.
6. Maher, A. R.; Al-Baghdad, S. 2004. Effect of compression ratio, equivalence ratio and engine speed on the performance and emission characteristics of a spark ignition

- engine using hydrogen as a fuel, *Renewable Energy* 29: 2245–2260.
<http://dx.doi.org/10.1016/j.renene.2004.04.002>.
7. **Gupta, S. K.; Mittal, M.** 2018. Assessing the effect of compression ratio on the performance, combustion and emission characteristics of a spark-ignition engine, and optimum spark advance at different operating conditions, SAE Technical Paper 2018-01-1668.
<http://dx.doi.org/10.4271/2018-01-1668>.
 8. **Shi, C.;** et al., 2020. Assessment of spark-energy allocation and ignition environment on lean combustion in a twin-plug Wankel engine, *Energy Conversion and Management* 209: 112597.
<https://doi.org/10.1016/j.enconman.2020.112597>.
 9. **Soylu, S.; Gerpen, J. Van.** 2004. Development of empirically based burning rate sub-models for a natural gas engine, *Energ. Conv. and Manag.* 45(4): 467–481.
[http://dx.doi.org/10.1016/S0196-8904\(03\)00164-X](http://dx.doi.org/10.1016/S0196-8904(03)00164-X).
 10. **Menacer, B.;** et al. 2017. The convection heat transfer rate evaluation of a 6-cylinder in-line turbocharged direct-injection diesel engine, *Mechanika* 23(4): 528-536.
<https://doi.org/10.5755/j01.mech.23.4.14898>.
 11. **Homdoun, N.; Tippayawong, N.; Dussadee, N.** 2015. Prediction of small spark ignited engine performance using producer gas as fuel, *Case Studies in Thermal Engineering* 5: 98-103.
<http://dx.doi.org/10.1016/j.csite.2015.02.003>.
 12. **Zheng, J. J. ;** et al. 2009. Effect of the compression ratio on the performance and combustion of a natural- gas direct-injection engine, *Proceedings of the institution of mechanical engineers, part d: Journal of automobile engineering* 223: 85–98.
<https://doi.org/10.1243%2F09544070JAUTO976>.
 13. **Olikara, C.; Borman, G. L.** 1975. A computer program for calculating properties of equilibrium combustion products with some applications to I. C. engines, SAE Technical, Paper no.750468.
<https://doi.org/10.4271/750468>.
 14. **Depcik, C.** 2000. Open-Ended Thermodynamic Cycle Simulation, M. S. Thesis, University of Michigan, Ann Arbor.
 15. **Ferentiet, I.** 2014. Research of some operating parameters and the emissions level variation in a spark ignited engine through on-board investigation methods in different loading conditions, *Central European Journal of Engineering* 4(2): 192– 208.
<http://dx.doi.org/10.2478/s13531-013-0167-9>.
 16. **Ferguson, C. R.** 1985. *Internal combustion engine, applied Thermosciences.* New York, NY: Wiley.
 17. **Gu, X.; Zuohua, H.; Wu, X.** 2012. Emission characteristics of a spark-ignition engine fuelled with gasoline-n-butanol blends in combination with EGR, *Fuel* 93: 611-617.
<https://doi.org/10.1016/j.fuel.2011.11.040>.
 18. **Arsie, I.;** et al. 1996. A Computer Code for the Optimal Design of S.I. Engine Control Strategies, SAE Paper 960359.
<https://doi.org/10.4271/960359>.
 19. **Gravalos, I.;** et al. 2013. Emissions characteristics of spark ignition engine operating on lower–higher molecular mass alcohol blended gasoline fuels, *Renewable Energy* 50: 27-32.
<https://doi.org/10.1016/j.renene.2012.06.033>.
 20. **Franzke, D. E.** 1981. Beitrag zur Ermittlung eines Klopfkriteriums der ottomotorischen Verbrennung und zur Vorausberechnung der Klopfgrenze. Thesis TU München.
 21. **Zapf, H.** 1969. Beitrag zur Untersuchung des Wärmeübergangs während des Ladungswechsels im viertakt-Dieselmotor, *MTZ* 30(12): 461-465.
 22. **Semin, A. R.; Nugroho, T. F.** 2010. Experimental and computational of engine cylinder pressure investigation on the port injection dedicated CNG engine development, *Journal of Applied Sciences* 10: 107-115.
<http://dx.doi.org/10.3923/jas.2010.107.115>.

B. Menacer, K. Naima, M. Bouchetara

NUMERICAL MODELLING OF EMISSION CHARACTERISTIC FOR A SINGLE CYLINDER SPARK IGNITION ENGINE

S u m m a r y

The main objective of this study is to elaborate an engine cycle simulation program using GT-Suite software to analyze the influence of equivalence ration and compression ratio on the main emissions of a four-stroke direct injection spark ignition engine. The experimental result is used to compare the cylinder pressure result obtained with the developed model. The present article is a study of the effect of compression ratio and equivalence ratio on the main emissions of the direct injection spark engine for a two-zone combustion analytical model and by using of the GT-Suite simulation software. The developed analytical model is validated by the use of experimental data. The analytical curve of the pressure in the combustion chamber is experimentally validated with a difference of the order of 6%.

Keywords: tow-zone model; hydrocarbons; carbon monoxide; nitrogen oxides; spark engine; GT-Suite software.

Received April 02, 2022

Accepted June 14, 2022



This article is an Open Access article distributed under the terms and conditions of the Creative Commons Attribution 4.0 (CC BY 4.0) License (<http://creativecommons.org/licenses/by/4.0/>).